(Received 27 May 2024, Accepted 19 July 2024, Scheduled 15 August 2024)

Reactively Loaded CPW Fed Dual Notched Pentagonal Ultrawide Band Antenna

Srijita Chakraborty[1,*], Narendra N. Pathak[2], and Mrinmoy Chakraborty[2]

[1] *Institute of Engineering & Management, Kolkata, India*
[2] *Dr. B.C. Roy Engineering College, Durgapur, India*

ABSTRACT: This research proposal includes the design of a unique coplanar waveguide (CPW) fed ultra-wideband (UWB) antenna prototype with dual notch band characteristics. The microstrip line fed antenna features a configuration of geometric slots, including a rectangle, a semi-circle slots, and a pentagonal stub, along with a microstrip feedline. The antenna measures 35.4 mm × 28.82 mm. Two notches are introduced at 5 to 5.8 GHz (14.8% bandwidth) and 7.2 to 7.8 GHz (8% bandwidth) by incorporating split ring resonators (SRRs) on the bottom surface. Aside from the dual stopbands for the WLAN band (5 to 5.8 GHz) and SHF satellite communication band (7.2 to 7.8 GHz), the designed antenna operates over an impedance bandwidth from 3 GHz to 11.2 GHz with voltage standing wave ratio (VSWR) below 2. The proposed antennas have been developed, prototyped, and successfully verified. Simulation data and measurement results are thoroughly examined and analyzed. To confirm the applicability of the antenna in pulsed communication systems, the correlation among the input signal of the transmission antenna with the output signal of the reception antenna in the time domain is estimated. This confirms that the antenna prototype is well suited for wireless communication applications in military radar systems, medical imaging, consumer electronics, and more.

1. INTRODUCTION

As the constraints of integrating various sub-systems in a single compact communication system emerge, the development of a UWB antenna with notch characteristics, as one of the fundamental microwave components and operational at multiple frequencies, is becoming significant. As Federal Communication Commission (FCC) unlicensed the UWB range from 3.1 Gigahertz to 10.6 Gigahertz, UWB wireless technology has gained a lot of momentum in research [1]. Square, circle [2], crescent [3], sectoral [4], ellipse [5], and their re-structured varieties are normally employed radiating patch structures in UWB planar antennas because they can be easily combined with microwave integrated circuits that are lightweight and have low profile in nature. Other applications such as WiMAX, WLAN, IEEE 802.16, IEEE 802.11a, and ITU-T frequency bands exist in the UWB spectrum. As a result, a UWB antenna with notched frequency responses is designed to reduce the likelihood of interference between narrowband and UWB systems.

In [6], a miniaturized antenna for ultra-wideband applications is presented. To achieve a compact size, the authors use a two-stage optimization process. First, a coarse-mesh electromagnetic simulation identifies promising initial designs with good signal return. Then, a more advanced optimization refines the design for excellent performance across the entire ultra-wideband range, within an overall dimension of 418 mm^2. In [7], a miniaturized ($22 \times 22\,mm^2$) circular slot antenna is presented for ultra-wideband communication (3–16 GHz). Designed for a common circuit board material (FR4), the antenna efficiently reflects minimal signal back across the entire usable frequency range (reflection coefficient below -10 dB), making it suitable for stable UWB applications. In [8], a modified U-shaped UWB antenna with a reverse T shaped slot is demonstrated. To ensure that the antenna efficiently transmits and receives signals across the UWB, the design incorporates a narrow strip in the patch and an inverted T-shaped slot in the ground plane. The paper verifies the antenna's performance through S-parameters (indicating good impedance matching) and radiation pattern analysis. In [9], a coplanar waveguide (CPW) fed UWB microstrip antenna is developed by loading an inverted L-strip. Simulations and real-world testing of the fabricated antenna ($25 \times 25 \times 1.6\,mm^3$) demonstrate good agreement, with the antenna achieving strong performance across a wide band (2.6–13.04 GHz) in terms of impedance matching, gain consistency, radiation patterns, and signal delay. In [10], a miniaturized antenna is reported for ultra-wideband applications (3–12.9 GHz) using a coplanar waveguide feed. The key to its wide bandwidth is a novel radiating structure with two asymmetric U-shaped strips and a staircase element. Despite its compact size ($23 \times 25.5 \times 1.6\,mm^3$), the antenna achieves excellent performance with a strong signal return, stable gain, and near-omnidirectional radiation, all confirmed by good agreement between simulations and real-world testing. In [11], a UWB antenna design based on a modified circular disc monopole is proposed. The design uses a three-step adjustment process on the ground plane to achieve a wide bandwidth (3.1–10.6 GHz) with good impedance matching. Testing confirms the antenna's effectiveness for UWB applications,

* Corresponding author: Srijita Chakraborty (srijita@iem.edu.in).

demonstrating a strong signal return (low VSWR), stable signal transmission and accurate signal reproduction (fidelity) across the band. In [12], an ultra-wideband (UWB) antenna design featuring a compact octagonal shape is illustrated. The authors simulated and built various prototypes as monopole antennas. These prototypes achieved good agreement between simulations and real-world testing, demonstrating their effectiveness for UWB applications with a wide-ranging frequency range (3.1 GHz to 14 GHz). In [13], an elliptical UWB antenna design uses a printed monopole structure. By modifying the shape of the ground plane, the authors achieve a wide operational bandwidth (3.1–10.6 GHz) despite the antenna's small size. Simulations and real-world testing confirm the antenna's performance, demonstrating good signal return, a near-omnidirectional radiation pattern, and faithful transmission of signal waveforms across the band. The paper also analyzes the antenna's ability to preserve signal integrity using a fidelity factor calculation. In [14], a UWB antenna is designed which consists of notched patch and bottom elements with a CPW feed. Designed and analyzed with HFSS software, the antenna achieves a wide bandwidth (3.083–11.0 GHz) with good signal transmission (VSWR < 2) and a maximum gain of around 5.7 dBi at 10 GHz, as verified by real-world measurements. In [15], a CPW fed UWB antenna is designed which comprises an open annulus shaped strip as ground and an open crescent shaped patch within the annulus as a radiation element. Despite its small size ($33 \times 30 \times 1.57$ mm), the design achieves an impressive ultrawide bandwidth, covering a frequency range of 3 to 14 GHz (129% relative bandwidth). In [16], notched bands are realized in a CPW fed UWB single iterated octagonal patch antenna by using split ring circular slots. Designed on a cost-effective FR4 substrate, the antenna features two independently controlled notched frequency bands (4 GHz–5.78 GHz and 6.83 GHz–8.22 GHz) achieved using split ring slots. An iterated octagonal CPW-fed patch antenna achieves a wide operating bandwidth (3.2–10.5 GHz) with good impedance matching. Simulations and measurements confirm excellent performance, including high efficiency ($> 90\%$), a compact size (20×23 mm^2), and a near-omnidirectional radiation pattern. In [17], a rose curve-contoured ultra-wideband antenna and dual notched band characteristics is developed using a complementary SRR in the antenna patch. The antenna achieves a wide bandwidth (3.1–11 GHz) in a very compact size (864 mm^3) on a common substrate. To prevent interference in Wi-Fi and ISM frequency bands (around 3.5 GHz and 5.8 GHz), the authors incorporate a special structure called a complementary dual-band split ring resonator near the antenna's feed line. In [18], an exponential tapering in a slotted ultra-wideband antenna is reported with notched features. The antenna is fed by a microstrip line loaded with special structures called Split Ring Resonators (SRRs). The study explores the versatility of this design by using two different SRR shapes (square and hexagon) to achieve the desired notch frequencies. The effectiveness of the design is confirmed by building and testing prototypes, with the measured performance (impedance and radiation) closely matching simulations. In [19], a microstrip-fed UWB circular patch antenna is designed for notch characteristics where a band-pass filter (BPF) based on a four-slotted line resonator and a stub integrated in circular radiating patch is developed. The filter itself is a compact design that effectively cancels unwanted signals (common-mode rejection) and features a clever feeding method to excite the desired signals. Additionally, small stubs are used to fine-tune the antenna's performance for good signal transmission (impedance matching) across a wide band (2.95–10.75 GHz). The design also includes a separate notch filter around 5.5 GHz achieved by strategically placed lines on the feed. Measurements confirm the effectiveness of the design for both differential and common-mode signals. In [20], a dual notched CPW-fed UWB antenna is demonstrated by implementing a π-shaped slot and electromagnetic bandgaps (EBGs). To achieve dual notches, the design incorporates electromagnetic EBGs on either side of the ground plane. These notches target specific bands for WiMAX, i.e., (3.3–3.7 GHz) and Satellite communication C-band, i.e., (6.5–7.2 GHz), while maintaining a wide operating bandwidth (2.7–11.7 GHz) with good signal transmission (VSWR < 2). The antenna was built and tested, demonstrating good agreement between simulations and real-world measurements. In [21], a coplanar waveguide fed convex dual notched hexagon shaped ultrawide band antenna is presented. The antenna utilizes an L-shaped ground plane and a tapered slot in the radiating patch to create two separate notches that block specific frequencies. This allows the antenna to operate in two UWBs (around 5.4 GHz and 9.6 GHz) while avoiding interference from common bands like PCS, GSM, and Wi-Fi. Despite its compact size ($40 \times 22 \times 1.6$ mm^3), the antenna achieves good impedance matching and exhibits acceptable radiation characteristics. In [22], a circular slotted UWB antenna fed by CPW, with dual band notch features is proposed by employing a stepped impedance stub within the radiation patch which is circular ring shaped and by implementing a parasitic element in arc shape within the patch. By adjusting the sizes of these elements, the antenna can reject signals at two specific frequencies while maintaining a wide operating bandwidth (2.7–11.6 GHz) with good signal transmission (VSWR < 2). The effectiveness of the design is confirmed through fabrication, measurements, and successful demonstration of the dual-band rejection functionality. In [23], a slotted dual notched UWB antenna is implemented using a rectangular slot and folding stepped resonator. To achieve the dual notches (3.76–5.9 GHz for Wi-Fi and 2.85–3.32 GHz for WiMAX), the design incorporates a rectangular slot on the patch and a folded stepped resonator in the ground plane. The antenna maintains a wide operating bandwidth (2.8–10.6 GHz) in a compact size (32×32 mm^2) and exhibits good performance in terms of signal transmission, signal delay, efficiency, and radiation patterns. In [24], a rectangular UWB antenna with a U-slot and a half-cut ground structure for dual notched feature has been proposed. To prevent interference in specific frequency bands (Wi-Fi and satellite), a U-shaped slot is etched into the radiator, creating dual notches (3.8–5.3 GHz and 6.2–7.3 GHz). The antenna maintains a consistent signal delay throughout the operational band (except for the notch regions) and exhibits good agreement between simulations and real-world testing, making it suitable for UWB applications. In [25], a radiating patch and ground plane slots are presented. The antenna uses a hexagonal radiating patch with two slots: a meandered S-shaped slot on

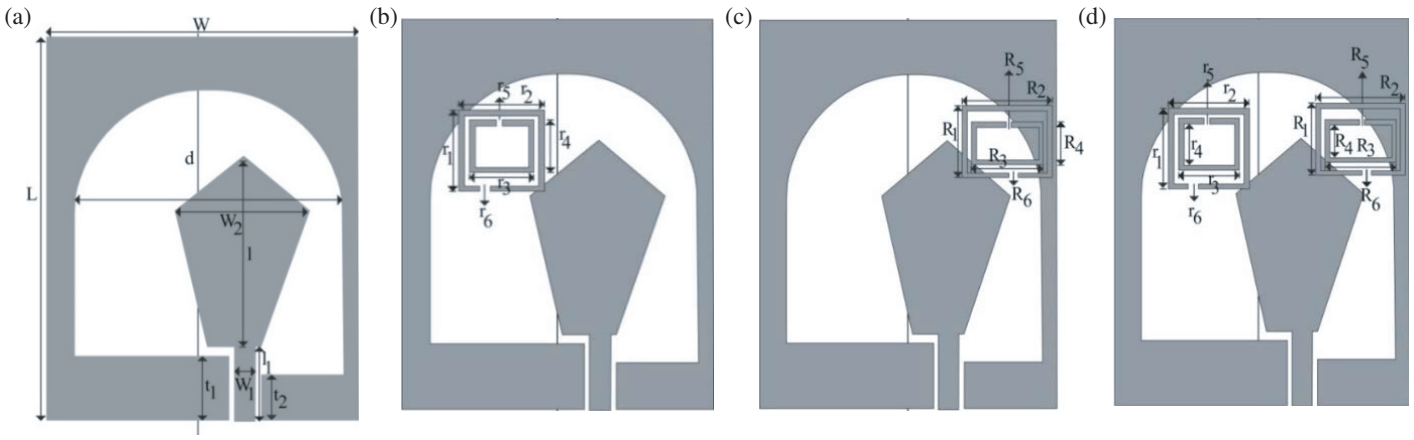

FIGURE 1. (a) UWB antenna (denoted as Antenna 1); (b) SRR loaded UWB antenna for WLAN band notch (denoted as Antenna 2); (c) SRR loaded UWB antenna for SHF Satellite Communication band notch (denoted as Antenna 3); (d) Optimized UWB antenna with dual notch characteristics(denoted as Antenna 4).

the patch for the WiMAX notch (3.2–3.8 GHz) and an inverted U-shaped slot in the ground plane for the WLAN notch (5.1–5.8 GHz). Despite a compact size ($44 \times 44\,\text{mm}^2$), the antenna achieves a wide operating bandwidth (2.4–12.4 GHz) and good agreement between simulations and real-world testing. Analysis of the current distribution on the antenna's surface confirms the effectiveness of the slots in creating the notches. In [26], an elliptical ultra-wideband antenna integrated with a reversed-U-shaped resonator and a conductor-shaped resonator is proposed with dual notched features. The UWB antenna achieves a wide bandwidth (2.5–11 GHz) with good performance (gain, phase response, group delay, radiation pattern) in a compact size. The notch variation utilizes strategically placed resonators to create dual notches that block WLAN and ITU bands while maintaining the UWB antenna's desirable characteristics. In [27], a miniaturized ($24 \times 20\,\text{mm}^2$) UWB antenna design with tunable notches is reported. The antenna uses a U-shaped radiating patch with structures (parasitic stubs and metamaterial elements) to achieve a wide operating bandwidth (2.7–11.4 GHz). Uniquely, the design incorporates two PIN diodes that can be switched to create four different functionalities: a regular UWB antenna, a UWB antenna with a notch for Wi-Fi (WLAN), a UWB antenna with a notch for S-band, or UWB antenna with notches for both S-band and Wi-Fi. The effectiveness of the design is confirmed through measurements in both frequency and time domains.

The demonstrated dual notch UWB antenna consists of regular geometric shapes of semicircular with rectangular slots and a pentagonal stub. The microstrip fed antenna has been designed and analyzed. The UWB frequency varies from 3 GHz to 11.2 GHz with VSWR less than 2. Systematic development of notch characteristics has been implemented in the proposed UWB antenna by incorporating SRRs to minimize existing interference from commercial application bands. The dual notch bands are introduced at WLAN band (i.e., 5 to 5.8 GHz, with 14.8% bandwidth percentage) and SHF satellite communication band (i.e., 7.2 to 7.8 GHz, with 8% bandwidth percentage). Explicit analysis on time domain of the designed antenna has been performed. The designed antenna is prototyped, and the measurements are in concurrence with simulation results. The novelty of the work lies in the implementation of resonators in the broad surface of the UWB antenna, due to which mutual coupling between the notch bands can be minimized. Also the notches exhibit independently controllable feature, which can be justified by studying the nature of independence of the notch bands. Loading of resonators in broad surface of the antenna provides provision for triple/quad notch realization in the same structure. Detailed analysis on time domain has been performed for the proposed dual notched antenna.

2. ANTENNA DESIGN

2.1. Systematic Development of UWB Antenna with Dual Notch Characteristics

The recommended UWB antenna has dimensions as given in Table 2 and is prototyped on an FR4 Epoxy dielectric substrate (ε_r i.e., dielectric constant = 4.4, tan δ i.e., loss tangent = 0.002, h i.e., thickness = 1.57 mm), as given in Figure 1(a) (Antenna 1). A CPW feed microstrip line, having a width of 1.98 mm for 50 Ω impedance, has been incorporated to excite the pentagonal stub. To obtain a notch band at WLAN band (i.e., 5 to 5.8 GHz) , a rectangular SRR has been integrated in the ground surface as demonstrated in Figure 1(b) (Antenna 2). Subsequently, to achieve notch band at SHF satellite communication band (i.e., 7.2 to 7.8 GHz), a second rectangular SRR is integrated in the lower surface of the proposed UWB antenna as given in Figure 1(c) (Antenna 3). To minimize the mutual coupling among the slot and resonators, the antenna is optimized to generate simultaneous dual notch band characteristics, as illustrated in Figure 1(d) (Antenna 4). The VSWR versus frequency variation for the proposed UWB antennas with notch characteristics are shown in Figure 2. Thus, the work focuses on the systematic development of a UWB dual notch band antenna to minimize interference from commercial application bands. The dual and notched UWB antenna has been modelled and simulated using different dielectric substrates, and a comparative analysis of the VSWR variation with respect to frequency for UWB antenna

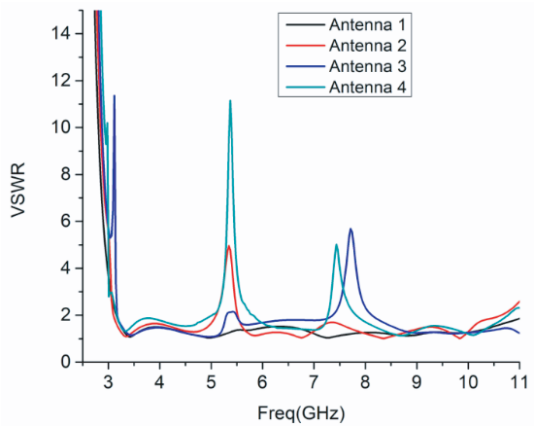

FIGURE 2. Comparative VSWR versus frequency variation of proposed antennas based on simulation data.

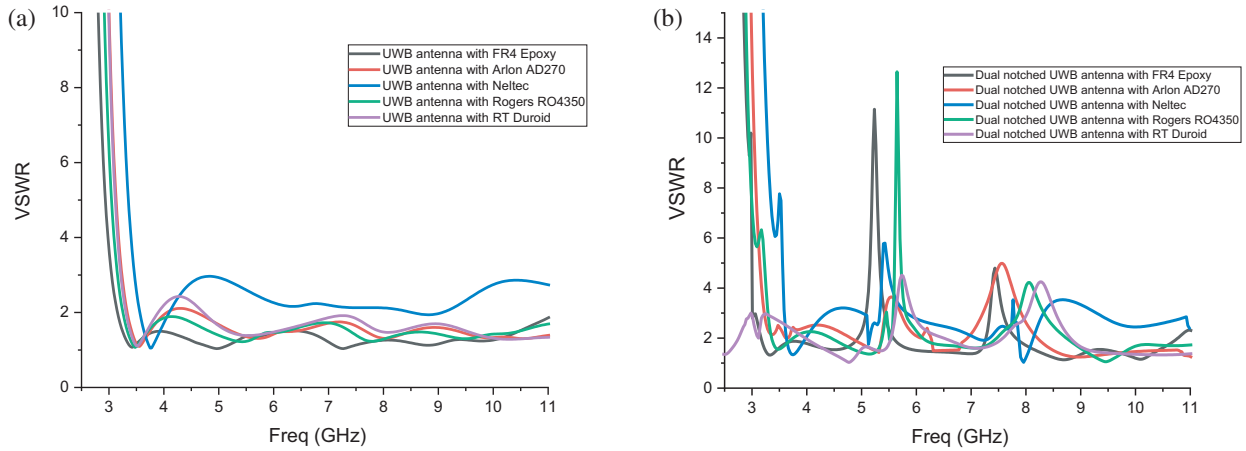

FIGURE 3. Comparative VSWR versus frequency variation for (a) Proposed ultrawide band antenna, (b) Dual band notched ultrawide band antenna, with different dielectric substrate based on simulation data.

and notched UWB antenna is illustrated in Figure 3. The various parameters for the dielectric substrate used for the comparison are FR4 Epoxy ($\varepsilon_r = 4.4$, $\tan\delta = 0.002$, $h = 1.57$ mm), Arlon AD270 ($\varepsilon_r = 2.7$, $\tan\delta = 0.0023$, $h = 1.58$ mm), Neltec ($\varepsilon_r = 3.2$, $\tan\delta = 0.0024$, $h = 0.76$ mm), Roger RO4350 ($\varepsilon_r = 3.66$, $\tan\delta = 0.004$, $h = 1.52$ mm), RT Duroid ($\varepsilon_r = 2.2$, $\tan\delta = 0.0009$, $h = 2$ mm).

Figure 2 illustrates the VSWR versus frequency variation of the notched UWB antenna. The antenna design methodology can be given as:

Step 1: The objective is to design a UWB antenna with dual notch band frequency for applications, including imaging, remote sensing, multimedia, localization, short-range, high-data-rate transmission, and radar.

Step 2: Based on mathematical modeling of resonators (Eqs. (1)–(8)), the antenna dimensions are calculated.

Step 3: Particle Swam Optimization algorithm has been used to optimize the parameters such as resonant frequency, VSWR, Length L, and width W of the antenna, for UWB antenna. Further, VSWR and width of the resonators r_2 and R_2 are optimized to achieve dual notch band UWB antenna. The optimizing range is given in Table 1.

TABLE 1. Parameter range of values.

Parameters for Antenna 1	Resonant Frequency	VSWR	L	W
Max	12 GHz	5	40 mm	30 mm
Min	2 GHz	0	30 mm	20 mm
Parameters for Antenna 4	**VSWR**	r_2	R_2	
Max	30	10 mm	10 mm	
Min	0	5 mm	5 mm	

Step 4: Particle Swam Optimization has been implemented using MATLAB software. The termination criterion is 60 iterations and less than or equal to 1 percent error in the cost function.

Step 5: Antenna 1 (UWB antenna) and Antenna 4 (dual notch band UWB antenna) have been designed and simulated with optimized parameters. It can be seen from Figure 3 that VSWRs are maximized at 5.5 GHz/7.5 GHz and minimized (< 2) in rest of the antenna frequency band to guarantee the fitness of the best designed antenna.

2.2. Parametric Analysis

An asymmetrical geometry [35, 36] is implemented for UWB antenna as shown in Figure 1 to achieve better performance. The pentagonal stub has been optimized to achieve the mid and higher frequency range, while left and right stepping along with the circular arc has been optimized to obtain the lower frequency range, as shown Figure 4. The VSWR is well below 2 in ultrawide frequency range of the asymmetrical antenna, as can be observed in Figure 2, which justifies the superior antenna performance.

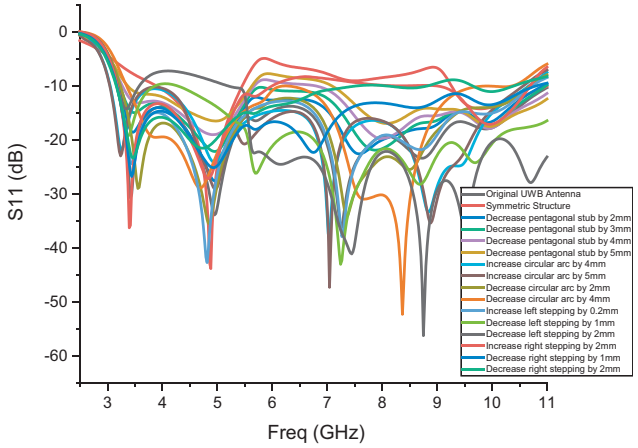

FIGURE 4. Variation of antenna parameters based on simulation data for realization of ultrawide band antenna.

Two SRRs are inserted on the bottom surface of the antenna to obtain dual notched bands at 5 GHz to 5.8 GHz (14.8%) and 7.2 GHz to 7.8 GHz (8%) GHz with the center frequencies 5.4/7.5 GHz, respectively. The band notched features may be controlled by appropriately altering the resonator specifications at the bottom surfaces of the antenna. The effective lengths of the resonators are in accordance with [28–30]. The notched bands are generated when radiations are suppressed around the resonant frequencies (within the bandwidth of the notches). Evaluating the current distribution provides a comprehensive understanding for the formation of notched bands. Figure 5 depicts the distribution of current of the antenna, indicating that current confinement is higher around the resonator which results in the notched frequency bands.

2.3. Mathematical Modelling of Resonator [31]

The dimensional details of a square SRR is shown in Figure 6. The notch frequency, f_{notch}, which corresponds to the resonating frequency f_r of a square SRR, is given by

$$f_{notch} = \frac{\omega_{notch}}{2\pi} = \frac{1}{2\pi}\sqrt{\frac{1}{L_1 C_1}} \tag{1}$$

where L_1 = equivalent inductance of split ring resonator. C_1 = equivalent capacitance of split ring resonator.

This equivalent capacitance, C_1, can be evaluated as in [30] and [32]:

$$C_1 = \frac{(C_o + C_{gap})}{2} \tag{2}$$

The split gappings are of identical dimensions $G_1 = G_2 = g$. Thus, the gap capacitances are equal which can be denoted as C_{gap}, and the distributed series capacitances are indicated by $C' = C'' = C_o$ [30]. Assuming the thickness of the metallic strip conductors as t_1, the gap capacitances can be calculated as,

$$C_{gap} = \frac{\varepsilon_o x t_1}{g} \tag{3}$$

The distributed capacitances $C' = C'' = C_o$ are also a function of the split ring gap dimensions g and the average ring dimension r_{AVG} and given as,

$$C_o = (4r_{AVG} - g)C'' \text{ where, } r_{AVG} = r_{ext} - x - \frac{y}{2} \tag{4}$$

C'' is the capacitance value per unit length and is formulated as [30, 32]

$$C'' = \frac{\sqrt{\varepsilon_r}}{c_Z} \tag{5}$$

where c = free space velocity of light and Z = the line characteristic impedance [33].

The resonating frequency of a square split ring resonator resulting in the notch bands at its resonance can be expressed as,

$$f_r = \frac{1}{2\pi\sqrt{L_1 C_1}} = \frac{1}{2\pi\sqrt{L_1[(2r_{AVG} - \frac{r}{2})C'' + \frac{\varepsilon_o x t_1}{2g}]}} \tag{6}$$

The equivalent inductance L_1 is given as [34],

$$L_1 = 0.0002 \times l \times \left(2.303 \log_{10}\frac{4l}{x} - \gamma\right) \text{ µH} \tag{7}$$

where $\gamma = 2.853$ for square loop. The evaluation of the wire length l is given as

$$l = 8r_{ext} - g \tag{8}$$

where, length l and thickness x are in mm.

Based on the above calculation, asymmetric SRRs have been employed in the present work to achieve the desired notching frequencies. From the results, it can be justified that asymmetric SRRs yielded a better notch band in terms of VSWR parameter in comparison to symmetric SRRs.

3. LUMPED CIRCUIT OF THE ULTRAWIDE BAND ANTENNA WITH DUAL NOTCH BANDS

The equivalent electrical circuit for the proposed antenna has been developed gradually and optimized to the input impedance of electromagnetic model. The UWB nature of an antenna is owing to a considerable number of distinct resonances that coincide with each other. The input impedance of the equivalent circuit model is precisely matched to the proposed antenna. The wideband frequency range for an UWB antenna is caused by numerous independent resonances that overlap with one another. Multiple RLC components connected in series are used to model the proposed UWB antenna using the same approach.

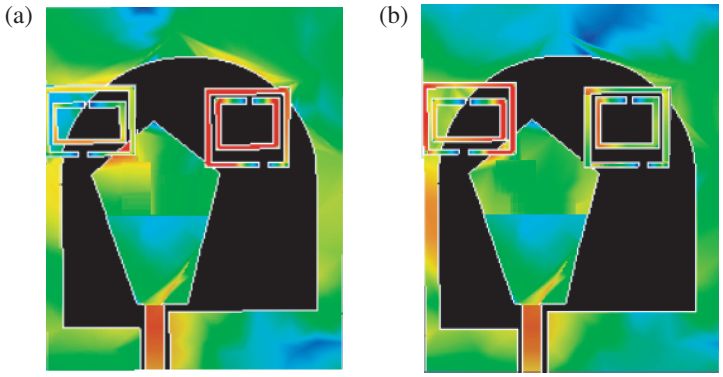

FIGURE 5. Simulated distribution of current for the dual notch band UWB antenna at 5.4/7.5 GHz as shown in (a) & (b).

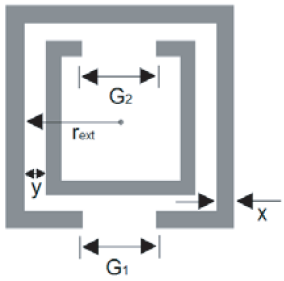

FIGURE 6. Dimensional details of Square SRR.

The values of the equivalent circuit model are determined by using Advance Design System (ADS).

For the resonant circuit, the values of the lumped circuit components are computed [37]. Eqs. (9), (10), and (11) provide formulas for calculating the values of L and C for the notch frequency.

Fractional Bandwidth:

$$\Delta = \frac{\omega_2 - \omega_1}{\omega_o} \tag{9}$$

The formulas for calculating values of L and C are:

$$L = \frac{Z_o \times L'}{\omega_o \times \Delta} \tag{10}$$

$$C = \frac{\Delta}{Z_o \times C' \times \omega_o} \tag{11}$$

where $Z_o = 50\,\Omega$, $L' = 0.3052$ and $C' = 1$ [37].

Equivalent circuit model for the recommended UWB antenna is given in Figure 7. The optimized circuit parameters are $L_0 = 0.42$ nH, $L_1 = 0.520$ nH, $L_2 = 0.26$ nH, $L_3 = 0.201$ nH, $L_4 = 0.106$ nH; $C_0 = 1.32$ pF, $C_1 = 4.164$ pF, $C_2 = 3.99$ pF, $C_3 = 2.404$ pF, $C_4 = 3.157$ pF, $R_1 = 46.03\,\Omega$, $R_2 = 55.4\,\Omega$, $R_3 = 39.19\,\Omega$, $R_4 = 53.92\,\Omega$. The results demonstrated in Figure 9(a) justify the fact that the S_{11} parameter of the equivalent circuit and the EM model of the UWB antenna are in concurrence.

The equivalent electrical circuit model developed for the dual notched band UWB antenna, shown in Figure 8, has optimized

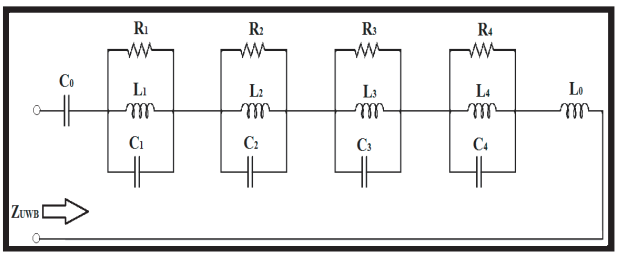

FIGURE 7. Equivalent electrical circuit ultrawide antenna.

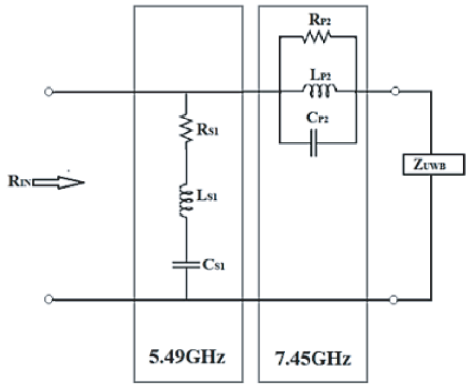

FIGURE 8. Equivalent circuit for the notched ultrawide band antenna.

circuit parameters as $L_{s1} = 1.53$ nH, $L_{p2} = 1.60$ nH; $C_{s1} = 0.54929$ pF, $C_{p2} = 0.28524$ pF; $R_{s1} = 11.6\,\Omega$, $R_{p2} = 67.4\,\Omega$. The results demonstrated in Figure 9(b) justify the fact that the S_{11} parameter of the equivalent circuit and the EM model of the dual notched ultrawide band antenna are in good agreement. The EM simulation VSWR and input impedance of the dual notched band antenna are also in sync with that of the circuit model as given in Figure 10.

4. NATURE OF NOTCHED FREQUENCY BAND INDEPENDENCE

Modification in the opening gap (as demonstrated in Figure 11) and width (as demonstrated in Figure 12) of the SRR 1 alters WLAN band. However, the other notch band remains almost intact as seen from figures. Likewise variations in the opening gap and width of SRR 2 yielded similar results, as seen in Figure 13 and Figure 14, respectively.

5. RESULTS AND DISCUSSION

Using a full-wave electromagnetic simulation tool, the proposed antenna was assessed and optimized. The antenna has been consequently prototyped as illustrated in Figure 15, with optimized structural parameters which are provided in Table 2.

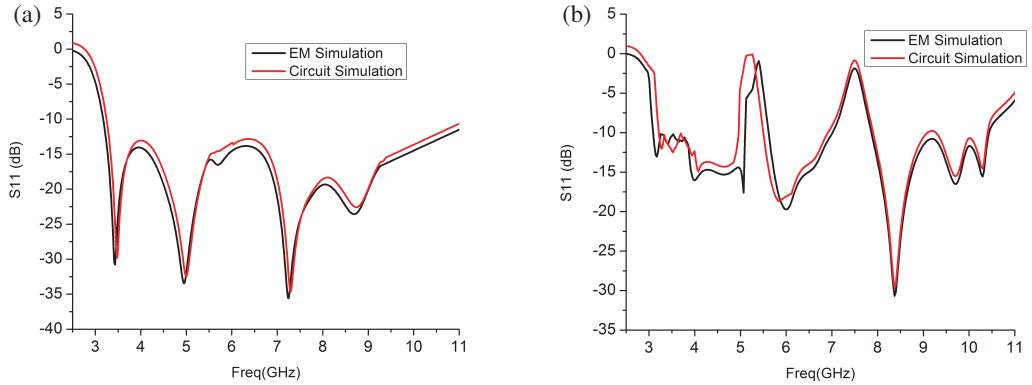

FIGURE 9. Comparative S parameter for full wave EM and circuit simulations. (a) Ultrawide band antenna. (b) Dual notched ultrawide band antenna.

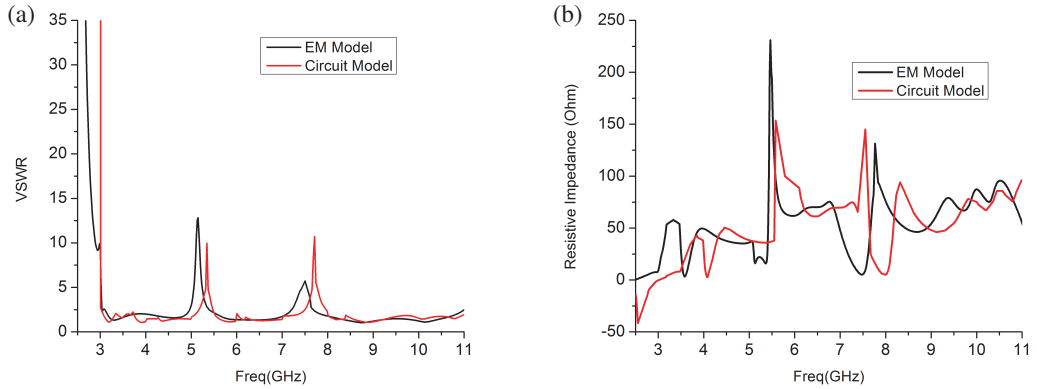

FIGURE 10. (a) VSWR variation against frequency. (b) Input impedance (z) variation against frequency of proposed ultrawide antenna.

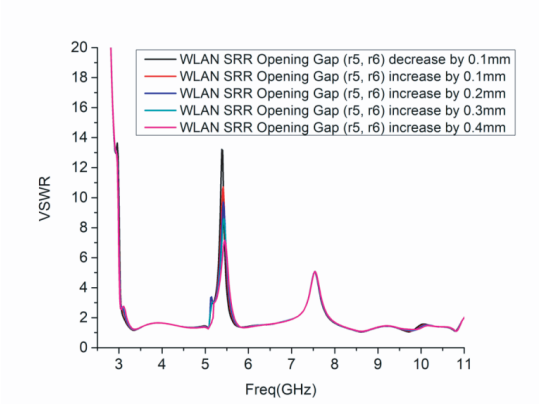

FIGURE 11. Variation of the opening gap of SRR for WLAN band.

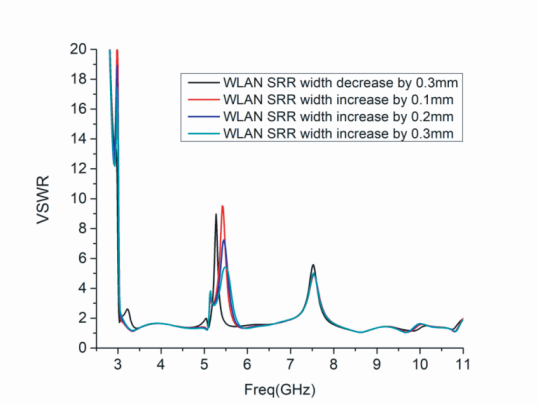

FIGURE 12. Variation of the width of SRR for WLAN band.

Figure 16 shows VSWR variation against frequency of the antenna, and from the figure it is evident that that the measurements are in sync with simulation results.

The overall antenna gain is shown in Figure 17. The highest gain achieved over the UWB range is around 2.7 dBi excluding the notched bands whereas the gain has been substantially decreased in the notch bands.

Figure 18 shows the normalised radiation pattern in YZ-XZ plane at 4/7/9 GHz. Excluding the notches, the antenna reports a stable omnidirectional pattern across the entire UWB spectrum. There is certain pattern deterioration observed at high frequencies which is owing to the extensive magnitude of the mode of higher order.

6. ANALYSIS OF ULTRAWIDE BAND ANTENNA PROTOTYPE IN TIME DOMAIN

Short pulse transmission is used in UWB impulse radio technology. Although the designed antenna has a broad response in frequency domain, it does not imply that it will perform well in the time domain. As a result, within an anechoic chamber, two identical antennas were placed on the dual port terminals of the

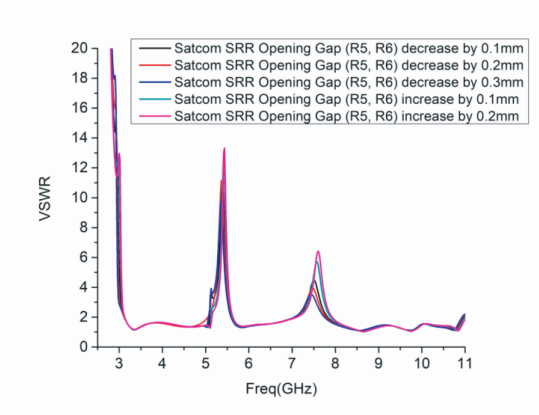

FIGURE 13. Variation of the opening gap of SRR for SHF satellite communication band.

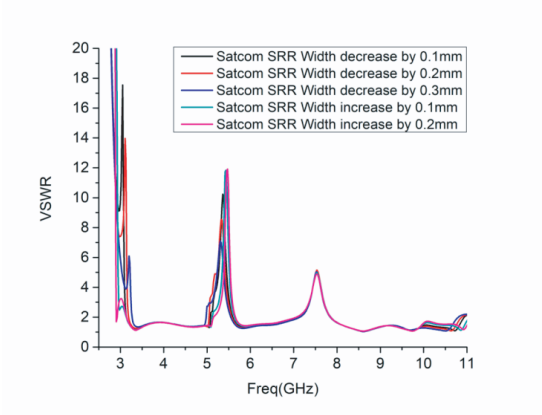

FIGURE 14. Variation of the width of SRR for SHF satellite communication band.

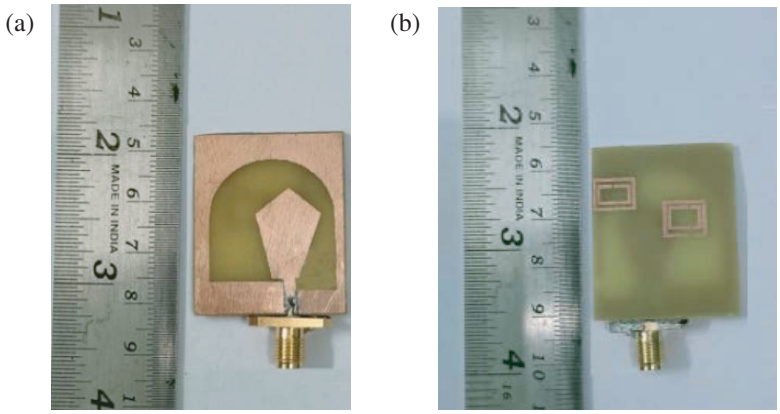

FIGURE 15. Antenna prototype with (a) Front view, (b) Rear view (units in millimeter).

TABLE 2. Antenna Dimensional details as shown in Figure 1.

Notation used in figure	Description	Dimension (in milimeter)	Notation used in figure	Description	Dimension (in milimeter)
L	Length of UWB antenna	35.4	r_3	Width of Inner SRR (SRR 1)	6.66
W	Width of UWB antenna	28.82	r_4	Length of Inner loop of SRR (SRR 1)	4.67
L	Length of pentagonal stub	17.64	r_5	Gap of Inner SRR (SRR 1)	0.57
W_2	Width of pentagonal stub	12.49	r_6	Gap of Outer loop of SRR (SRR 1)	1.5
D	Diameter of semicircle	24.56	R_1	Length of Outer SRR (SRR 2)	6.58
t_1	Left stepping of UWB antenna	5.94	R_2	Width of Outer loop of SRR (SRR 2)	8.76
t_2	Right stepping of UWB antenna	4.24	R_3	Width of Inner SRR (SRR 2)	6.76
l_1	Length of microstrip feedline	6.89	R_4	Length of Inner loop of SRR (SRR 2)	3.88
W_1	Width of microstrip feedline	1.98	R_5	Gap of Inner SRR (SRR 2)	0.46
r_1	Length of Outer SRR (SRR 1)	7.37	R_6	Gap of Outer loop of SRR (SRR 2)	0.4
r_2	Width of Outer loop of SRR (SRR 1)	8.66			

analyzer to confirm the applicability of the proposed notched UWB antenna for time domain applications as well as to quantify group delay. The two similar antennae function as transmission antenna and reception antenna respectively. When the antennas are placed face to face, from a particular direction, the front side of the first antenna and the rear side of the second antenna will be visible (as observed from Figure 19). In the front side, the patch and ground planes are visible, and in the rear side, the two split ring resonators, integrated in the rear side of the antenna substrate are visible [38]. To improve measurement

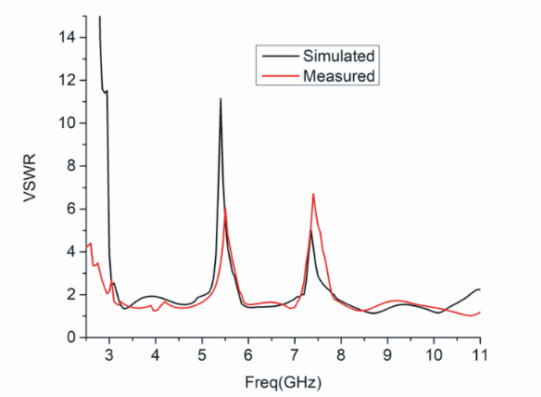

FIGURE 16. VSWR of the proposed antenna based on simulation and measurement data.

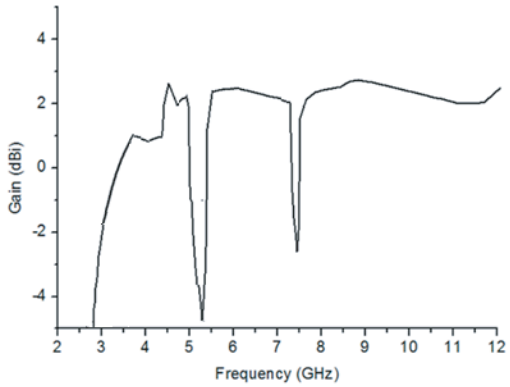

FIGURE 17. Gain versus frequency of the proposed dual notched ultra-wide band antenna.

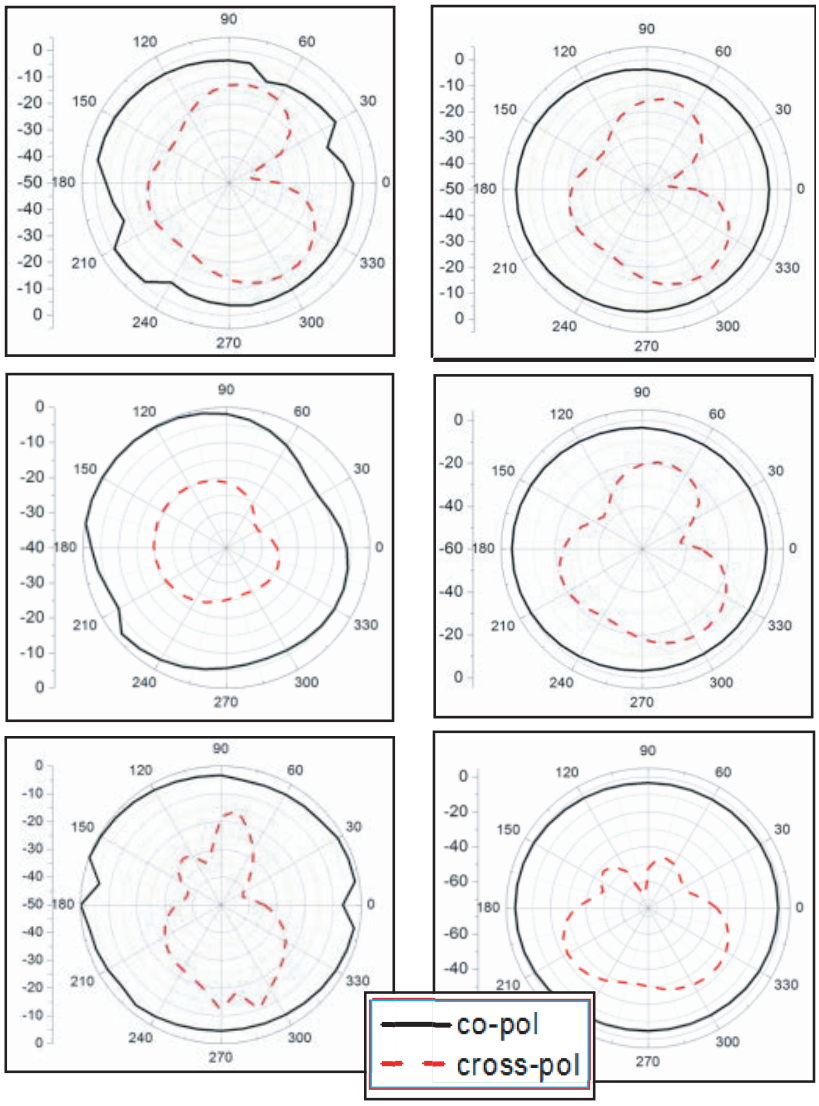

FIGURE 18. Radiation profile of the dual notched ultrawide band antenna at 4 GHz/7 GHz/9 GHz.

precision, the planes of reference were adjusted with respect to the terminals of the antenna. The measured transfer function or transmission loss of two identical types of fabricated antennas positioned facing each other and side by side in free space at 30 centimeter and 60 centimeter distances is demonstrated in Figure 19. The S_{21} is observed to decrease as the distance

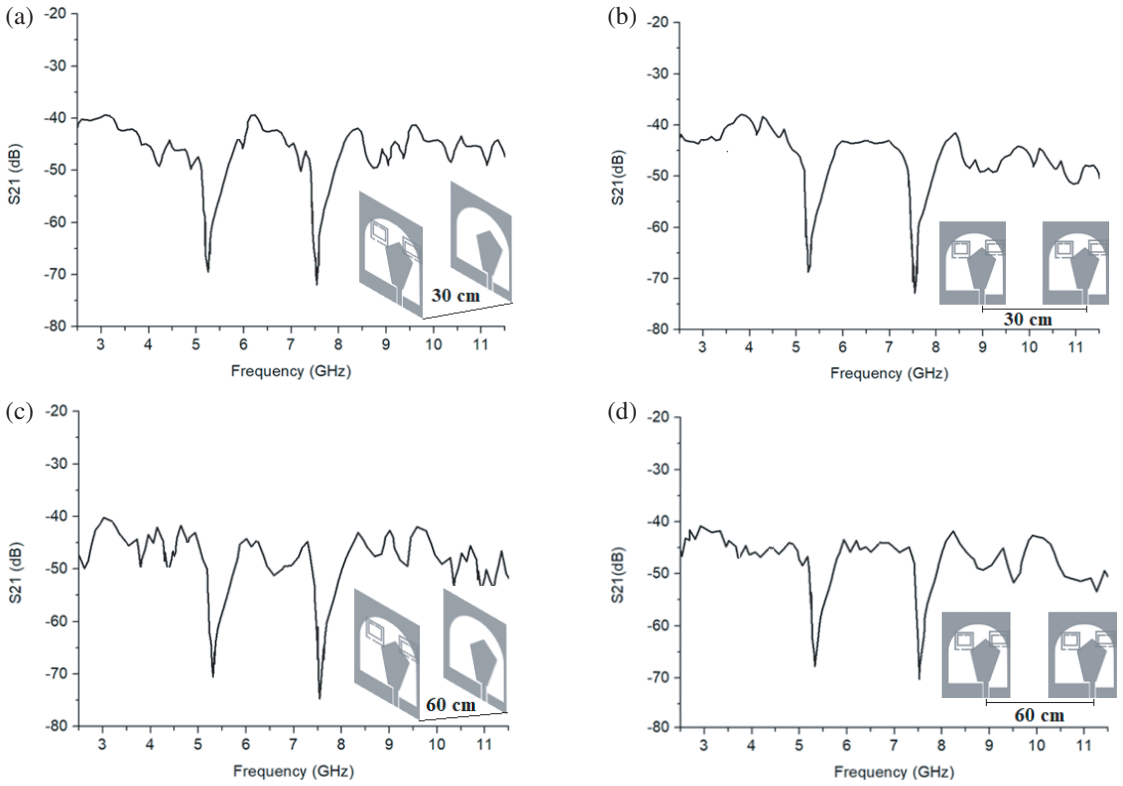

FIGURE 19. Transmission loss versus frequency of two identical UWB antennae in (a) facing each other at 30 cm, (b) Side by side at 30 cm, (c) facing each other at 60 cm, (d) Side by side at 60 cm.

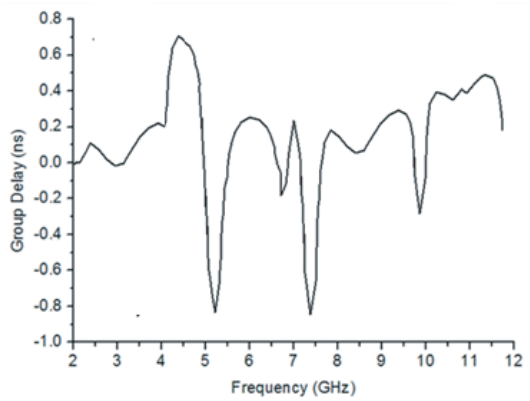

FIGURE 20. Group delay versus frequency of the antenna prototype.

between the antennas widens. A relatively constant response with minor non-linearity ensures that the broadcast signal is received without distortion. Measured group delay is identified to ensure that UWB antenna is free from distortion. The variance in group delay is within one nano second, excluding the dual notched frequency band, where it is much larger, as illustrated in Figure 20. This implies that the antenna is devoid of distortion and has notable time domain features in the operational range.

By definition, the correlation coefficient (denoted by ρ) is:

$$\rho = \max \tau \left[\frac{\int S_1(t) S_2(t-\tau) dt}{\sqrt{\int S_1^2(t) dt} \sqrt{\int S_2^2(t) dt}} \right] \qquad (12)$$

where $S_1(t)$ and $S_2(t)$ are signals of transmission antenna and reception antenna, and 'τ' is the delay.

If $\rho = 1$, fidelity has reached a maximum level, implying that the broadcast and receiving signals are perfectly matched. It reflects two identical signal waveforms, and the antenna system does not degrade the input signal. The correlation coefficient for face-face position and side-side position is 0.853 and 0.871, respectively for the proposed UWB antenna; for notched antenna, the value of correlation coefficient is 0.827 and 0.837, respectively for face-face position and side-side position, respectively [38].

Table 3 shows a comparison with the relevant research. This comparative study was conducted based on feeding mechanism (CPW vs. Microstrip), notching technique, and quantity of

TABLE 3. Comparative study of proposed design with related literature.

Reference	Feeding Mechanism	Notching Technique	Notches	Size	Bandwidth	Application	Time Domain Analysis	Equivalent Circuit Model	Mathematical Modelling of resonators
[16]	CPW fed	Split ring circular slots	4 to 5.78 GHz, 6.83 to 8.22 GHz	23 × 20 ×1.6 mm^3	3.2–10.5 GHz	UWB range without WLAN band and X-band	×	×	×
[17]	CPW fed	Complementary dual-band SRR	3.5 and 5.8 GHz	864 mm^3	3.1–11 GHz	UWB range without Wi-Fi and ISM frequency bands	×	×	√
[18]	Microstrip feedline	Square and hexagon SRRs	6.28 GHz/7.33 GHz (Tunable) 4.27 GHz and 6.1 GHz (Simultaneous)	29 × 55.8 ×1.52 mm^3	3.1–10.6 GHz	UWB range without 4.27 GHz and 6.1 GHz	×	×	×
[19]	Microstrip feedline	Dual spur-lines embedded in Microstrip feedline	5.5 GHz	29.38 × 28.25 × 0.508 mm^3	2.95–10.75 GHz	UWB range without 5.5 GHz	×	×	×
[20]	CPW fed	π-shaped slot and EBG	3.4 GHz (3.3 to 3.7 GHz) and 6.9 GHz (6.5 to 7.2 GHz)	40 × 52 × 0.7 62 mm^3	2.7–11.7 GHz	UWB range without S-band WiMAX application and C-band IEEE INSAT applications	×	×	√
[21]	CPW fed	L-shaped ground and stepped rectangular slot in patch	2.4 GHz and 7 GHz	40 × 22× 1.6 mm^3	3.17–10.67 GHz	UWB range without PCS, GSM 800/1900, ISM, WLAN, and X-band satellite uplink and downlink communicat ion system	×	×	×
[22]	CPW fed	Stepped impedance resonator and parasitic element in arc shape	5.5 GHz and 8 GHz	32 × 24 ×1.6 mm^3	2.7 to 11.6 GHz	UWB range without WLAN band and X-band	×	×	×
[23]	CPW fed	Rectangular slot and folding stepped resonator	5.2 GHz and 3.2 GHz	32 × 32 × 1.6 mm^3	2.8 to 10.6 GHz	UWB range without WLAN and Wimax	×	×	×
[24]	CPW fed	Rectangular slot	3.8 to 5.3 and 6.2 to 7.3 GHz	40 × 30 × 1.6 mm^3	2.6 to 10.6 GHz	UWB range without 3.8 to 5.3 and 6.2 to 7.3 GHz	√	×	×
[25]	CPW fed	S and U shaped Slots	3.2–3.8 GHz and 5.1–5.8 GHz	44 × 44 ×1.524 mm^3	2.4–12.4 GHz	UWB range without WLAN and Wimax	×	×	×
[26]	CPW fed	Inverted-U-shaped and conductor-shaped resonator	5.2–5.7 GHz and 7.2–8.5 GHz	24×32×1.5 mm^3	2.5–11GHz	UWB range without WLAN and ITU band	√	×	√
[27]	CPW fed	PIN diodes	2.85–3.34 GHz and 4.9–5.64 GHz	24 × 20 × 0.787 mm^3	2.7 to 11.4 GHz	UWB range without S-band and WLAN	√	×	×
Present	CPW fed	SRR	5 to 5.8 GHz and 7.2 to 7.8 GHz	35.4 × 28.82 ×1.57 mm^3	3 to 11.2 GHz	UWB range without WLAN band and the SHF satellite communication band	√	√	√

notches, size, frequency bandwidth, and application. The novelty of the work in comparison to other available articles lies in achieving well balanced and precise notch band characteristics. Further more time domain analysis, realization of equivalent circuit model, and mathematical modeling of resonators have been performed for the recommended antenna.

7. CONCLUSION

A wide range of wireless applications, including imaging, remote sensing, multimedia, localization, short-range, high-data-rate transmission, and radar, have benefited greatly from the development of ultra-wideband technology. A dual band notched UWB antenna is demonstrated in this research work. The WLAN (i.e., 5 to 5.8 GHz) and SHF satellite communication systems (i.e., 7.2 to 7.8 GHz) are developed employing SRRs. It is established that notches can be tuned exclusively, implying that altering the parameter of resonator only impacts the notch band and has no effect on the rest of UWB frequency. Experimental and simulated findings are in accordance. Within UWB, except at notch bands, constant amplitude of group delay and transfer function are obtained, resulting in excellent linear transmission of the antenna. This proposed dual notched UWB antenna is suitable for widespread application in emerging technology domains such as material sensors and imaging in the UWB range except WLAN and SHF satellite communication system frequency bands.

ACKNOWLEDGEMENT

The researchers are grateful for the assistance of AICTE funded IDEA Labs, BCREC, Durgapur, India, and extend gratitude to all concerned.

REFERENCES

[1] Federal Communications Commission, "Revision of part 15 of the commission's rules regarding ultra-wideband transmission system from 3.1 to 10.6 GHz," 98–153, ET Docket, Federal Communications Commission, Washington, DC, 2002.

[2] Ray, K. P., "Design aspects of printed monopole antennas for ultra-wide band applications," *International Journal of Antennas and Propagation*, Vol. 2008, 2008.

[3] Azenui, N. C. and H. Y. D. Yang, "A printed crescent patch antenna for ultrawideband applications," *IEEE Antennas and Wireless Propagation Letters*, Vol. 6, 113–116, 2007.

[4] Ray, K. P., S. S. Thakur, and R. A. Deshmukh, "UWB printed sectoral monopole antenna with dual polarization," *Microwave and Optical Technology Letters*, Vol. 54, No. 9, 2066–2070, 2012.

[5] Huang, C.-Y. and W.-C. Hsia, "Planar elliptical antenna for ultra-wideband communications," *Electronics Letters*, Vol. 41, No. 6, 296–297, 2005.

[6] Koziel, S. and A. Bekasiewicz, "A structure and simulation-driven design of compact CPW-fed UWB antenna," *IEEE Antennas and Wireless Propagation Letters*, Vol. 15, 750–753, 2015.

[7] Mohsen Hosseini Varkiani, S., M. Afsahi, and P. Reazaie, "Circular slot CPW-fed monopole antenna for UWB applications," *Microwave and Optical Technology Letters*, Vol. 56, No. 8, 1773–1776, Aug. 2014.

[8] Choe, H. and S. Lim, "Ultrawideband compact U-shaped antenna with inserted narrow strip and inverted T-shaped slot," *Microwave and Optical Technology Letters*, Vol. 56, No. 10, 2265–2269, Oct. 2014.

[9] Gautam, A. K., S. Yadav, and B. K. Kanaujia, "A CPW-fed compact UWB microstrip antenna," *IEEE Antennas and Wireless Propagation Letters*, Vol. 12, 151–154, 2013.

[10] Tang, Z. J., J. Zhan, and H. L. Liu, "Compact CPW-fed antenna with two asymmetric U-shaped strips for UWB communications," *Electronics Letters*, Vol. 48, No. 14, 810–812, Jul. 2012.

[11] Gao, G. P., M. K. Yang, S. F. Niu, and J. S. Zhang, "Study of a novel U-shaped monopole UWB antenna by transfer function and time domain characteristics," *Microwave and Optical Technology Letters*, Vol. 54, No. 6, 1532–1537, Jun. 2012.

[12] Bithikh, M., R. Aksas, H. Kimouche, and A. Azrar, "New UWB antenna design for wireless communications," *Microwave and Optical Technology Letters*, Vol. 54, No. 3, 692–697, Mar. 2012.

[13] Karimabadi, S. S. and A. R. Attari, "Compact and ultra wideband printed eliptical monopole antenna with modified-shape ground plane," *Microwave and Optical Technology Letters*, Vol. 51, No. 11, 2604–2607, Nov. 2009.

[14] Maeng, J. H., Y. J. Lee, and W. G. Yang, "Design and implementation of UWB CPW-fed planar monopole antenna," *Microwave and Optical Technology Letters*, Vol. 51, No. 3, 650–653, Mar. 2009.

[15] Chen, M.-E. and J.-H. Wang, "CPW-fed crescent patch antenna for UWB applications," *Electronics Letters*, Vol. 44, No. 10, 613–615, May 2008.

[16] Awan, W. A., A. Zaidi, N. Hussain, A. Iqbal, and A. Baghdad, "Stub loaded, low profile UWB antenna with independently controllable notch-bands," *Microwave and Optical Technology Letters*, Vol. 61, No. 11, 2447–2454, 2019.

[17] Safia, O. A., M. Nedil, L. Talbi, and K. Hettak, "Coplanar waveguide-fed rose-curve shape UWB monopole antenna with dual-notch characteristics," *IET Microwaves, Antennas & Propagation*, Vol. 12, No. 7, 1112–1119, 2018.

[18] Saha, C., P. Natani, L. A. Shaik, J. Y. Siddiqui, and Y. M. M. Antar, "Square/hexagonal split ring resonator loaded exponentially tapered slot ultra wideband (UWB) antenna with frequency notch characteristics," *Microwave and Optical Technology Letters*, Vol. 59, No. 6, 1241–1245, Jun. 2017.

[19] Lee, C.-H., J.-H. Wu, C.-I. G. Hsu, H.-L. Chan, and H.-H. Chen, "Balanced band-notched UWB filtering circular patch antenna with common-mode suppression," *IEEE Antennas and Wireless Propagation Letters*, Vol. 16, 2812–2815, 2017.

[20] Peddakrishna, S. and T. Khan, "Design of UWB monopole antenna with dual notched band characteristics by using π-shaped slot and EBG resonator," *AEU — International Journal of Electronics and Communications*, Vol. 96, 107–112, 2018.

[21] Shinde, P. N. and B. K. Mishra, "Compact thin ground plane UWB antenna with dual band stop characteristics," *Microwave and Optical Technology Letters*, Vol. 55, No. 5, 1045–1049, 2013.

[22] Li, Y., W. Li, and R. Mittra, "Miniaturized CPW-FED UWB antenna with dual frequency rejection bands using stepped impedance stub and arc-shaped parasitic element," *Microwave and Optical Technology Letters*, Vol. 56, No. 4, 783–787, 2014.

[23] Rao, P. S., B. S. H. Prasad, J. Kavitha, and U. Jayaram, "A multislot UWB monopole antenna with dual band notch characteristics," *Progress In Electromagnetics Research C*, Vol. 138, 79–90, 2023.

[24] Subhash, B. K. and R. C. Biradar, "A rectangular slotted dual-notch UWB antenna for wireless communication application," *Telecommunications and Radio Engineering*, Vol. 83, No. 2, 27–36, 2024.

[25] Mukherjee, S., A. Roy, S. Maity, T. Tewary, P. P. Sarkar, and S. Bhunia, "Design of dual band-notched UWB hexagonal printed microstrip antenna," *International Journal of Microwave and Wireless Technologies*, Vol. 15, No. 3, 526–534, 2023.

[26] Kumar, O. P., T. Ali, P. Kumar, P. Kumar, and J. Anguera, "An elliptical-shaped dual-band UWB notch antenna for wireless applications," *Applied Sciences*, Vol. 13, No. 3, 1310, 2023.

[27] Sreelakshmi, K. and G. S. Rao, "A compact reconfigurable CPW-fed dual band-notched UWB antenna using PIN diodes," *Iranian Journal of Science and Technology, Transactions of Electrical Engineering*, Vol. 47, No. 3, 1153–1165, 2023.

[28] Siddiqui, J. Y., C. Saha, and Y. M. M. Antar, "Compact SRR loaded UWB circular monopole antenna with frequency notch characteristics," *IEEE Transactions on Antennas and Propagation*, Vol. 62, No. 8, 4015–4020, 2014.

[29] Saha, C., J. Y. Siddiqui, and Y. M. M. Antar, *Multifunctional Ultrawideband Antennas: Trends, Techniques and Applications*, CRC Press, 2019.

[30] Saha, C., J. Y. Siddiqui, and Y. M. M. Antar, "Square split ring resonator backed coplanar waveguide for filter applications," in *2011 XXXth URSI General Assembly and Scientific Symposium*, 1–4, Istanbul, Turkey, Aug. 2011.

[31] Siddiqui, J. Y., C. Saha, C. Sarkar, L. A. Shaik, and Y. M. M. Antar, "Ultra-wideband antipodal tapered slot antenna with integrated frequency-notch characteristics," *IEEE Transactions on Antennas and Propagation*, Vol. 66, No. 3, 1534–1539, 2018.

[32] Siddiqui, J. Y., C. Saha, and Y. M. M. Antar, "Compact SRR loaded UWB circular monopole antenna with frequency notch characteristics," *IEEE Transactions on Antennas and Propagation*, Vol. 62, No. 8, 4015–4020, 2014.

[33] Bahl, I. and P. Bhartia, *Microwave Solid State Circuit Design*, John Wiley & Sons, 1998.

[34] Terman, F. E., *Radio Engineers' Handbook*, Mcgraw-Hill, 1943.

[35] Gunamony, S. L., G. J. Bala, S. M. G. Raj, and C. B. Pratap, "Asymmetric coplanar strip-fed electrically small reconfigurable 5G mid-band antenna," *International Journal of Communication Systems*, Vol. 34, No. 15, e4935, 2021.

[36] Alam, M. M., R. Azim, N. M. Sobahi, A. I. Khan, and M. T. Islam, "An asymmetric CPW-fed modified bow tie-shaped antenna with parasitic elements for ultra-wideband applications," *International Journal of Communication Systems*, Vol. 35, No. 9, e5130, 2022.

[37] Ellis, M. S., P. Arthur, A. R. Ahmed, J. J. Kponyo, B. Andoh-Mensah, and B. John, "Design and circuit analysis of a single and dual band-notched UWB antenna using vertical stubs embedded in feedline," *Heliyon*, Vol. 7, No. 12, e08554, 2021.

[38] Ghatak, R., B. Biswas, A. Karmakar, and D. Poddar, "A circular fractal UWB antenna based on descartes circle theorem with band rejection capability," *Progress In Electromagnetics Research C*, Vol. 37, 235–248, 2013.